

Supporting Information

Carbazole functionalized new bipolar ligand for monochromatic red light emitting Europium(III) complex: combined experimental and theoretical study

B. Rajamouli,^a C. S. Dwaraka Viswanath,^b S. Giri,^a C. K. Jayasankar,^b and V. Sivakumar^{a,*}

^a Department of Chemistry, National Institute of Technology Rourkela, Rourkela-769 008, Odisha, India.

^b Department of Physics, Sri Venkateswara University, Tirupati-517 502, Andhrapradesh, India.

* To whom correspondence should be addressed. Email: vsiva@nitrkl.ac.in (V. Sivakumar) Tel: +91-661-2462654.

Contents

1. **Scheme S1** Synthetic route of CBZ attached triphenyl functionalized ligand intermediates.
2. **Fig. S1** ground state optimized structures of the ligand.
3. **Fig. S2** ^1H (up), ^{13}C (middle) and ^{19}F -NMR (down) of Phen-FI-TPA-CBZ ligand.
4. **Fig. S3** The mass spectrum of the ligand, Phen-FI-TPA-CBZ.
5. **Fig. S4** The mass spectrum of the complex, $\text{Eu}(\text{TtA})_3\text{Phen-FI-TPA-CBZ}$.
6. **Fig. 5** FT-IR spectra of the ligand, corresponding $\text{Eu}(\text{III})$ -complex and $\text{Eu}(\text{tta})_3(\text{H}_2\text{O})_2$.
7. **Table ST1** The foremost Infrared frequencies (wavenumber in cm^{-1}) at room temperature for free ligand, its corresponding $\text{Eu}(\text{III})$ -complex and $\text{Eu}(\text{tta})_3(\text{H}_2\text{O})_2$.
8. **Fig. S6** The PXRD of the Phen-FI-TPA-CBZ ligand and corresponding $\text{Eu}(\text{III})$ complex.
9. **ST2.** The PXRD data's of $\text{Eu}(\text{III})$ complex.
10. **Fig. S7** TG- analysis curves for the ligand and its corresponding $\text{Eu}(\text{III})$ complex.
11. **Fig. S8** The band gap for the ligands and their corresponding $\text{Eu}(\text{III})$ complexes are calculated from diffuse reflectance spectra.
12. **Fig. S9** The PL excitation and emission spectra of Phen-FI-TPA-CBZ with different excitation and emission wavelengths.
13. **Fig. S10** The solvent effect of Phen-FI-TPA-CBZ of PL excitation (left) and emission (right) in different solvents.
14. **Fig. S11** Stokes shift $\Delta\bar{\nu}$ of Phen-FI-TPA-CBZ (right) versus the Lippert solvent parameter $\Delta f = f(\epsilon) - f(n^2)$ (The numbers refer to the solvents in Table S1). The straight line represents the linear fit to the 10 data points.
15. **Table ST3** PL spectral data of ligands in various solvents.
16. **Fig. S12** The obtained HOMO-LUMO of the ligand.

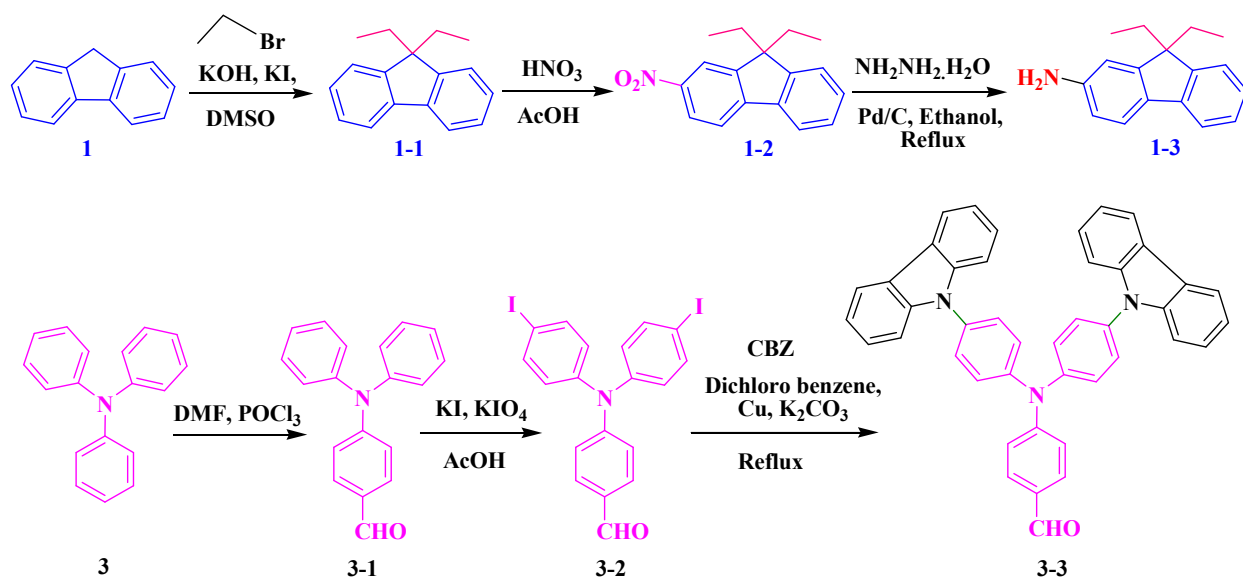
17. Fig. S13 The UV-Vis absorption spectra of Eu(TTA)₃Phen-FI-TPA-CBZ and its ligand in thin film and solid.

18. Fig. S14 The Phen-FI-TPA-CBZ ligand absorption spectra theoretically calculated.

19. Fig. S15 The energy levels of the ligand as well as Eu(III) complex arrangement.

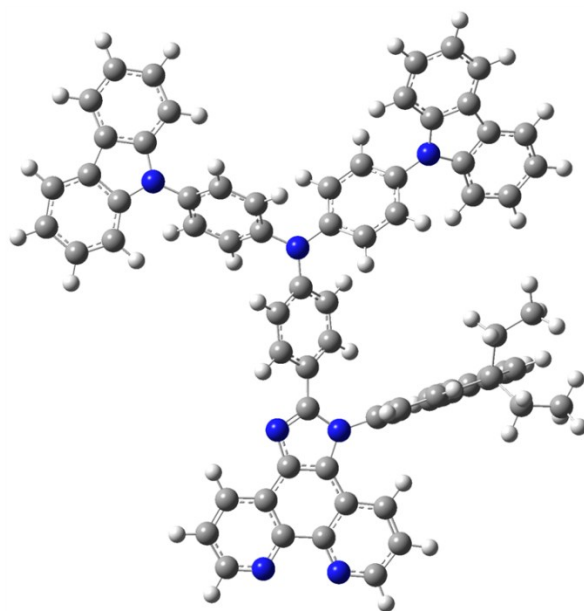
20. Fig. S16 The emission of the ligand (Phen-FI-TPA-CBZ) and UV-vis absorption spectra of TTA at Room-temperature.

21. References



Scheme S1 Synthetic route of CBZ attached triphenyl functionalized ligand intermediates.

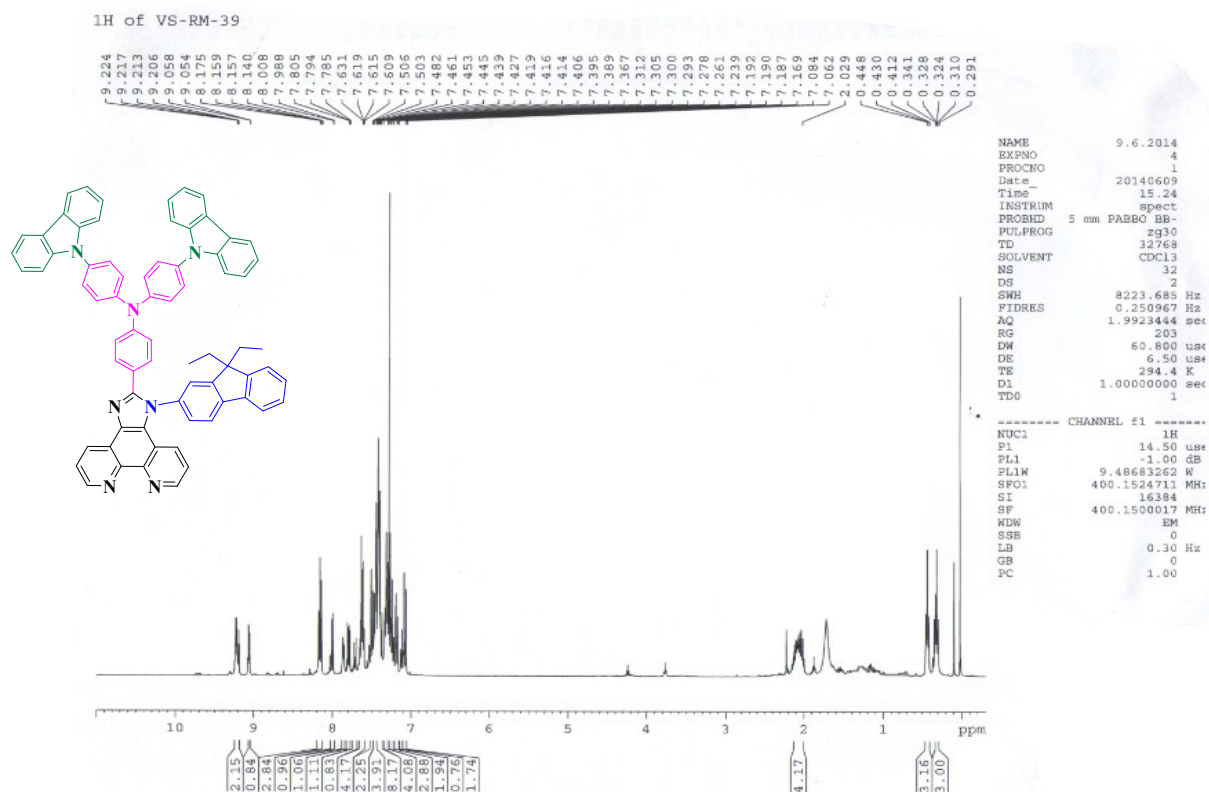
The synthesis of the intermediates, 9,9-diethyl-9H-fluorene (1-1)^[1,2] 9,9-diethyl-2-nitro-9H-fluorene (1-2)^[3] (diphenylamino)benzaldehyde (3-1),^[4] 4-(bis(4-iodophenyl)amino)benzaldehyde (3-2) are synthesized by reported literatures.

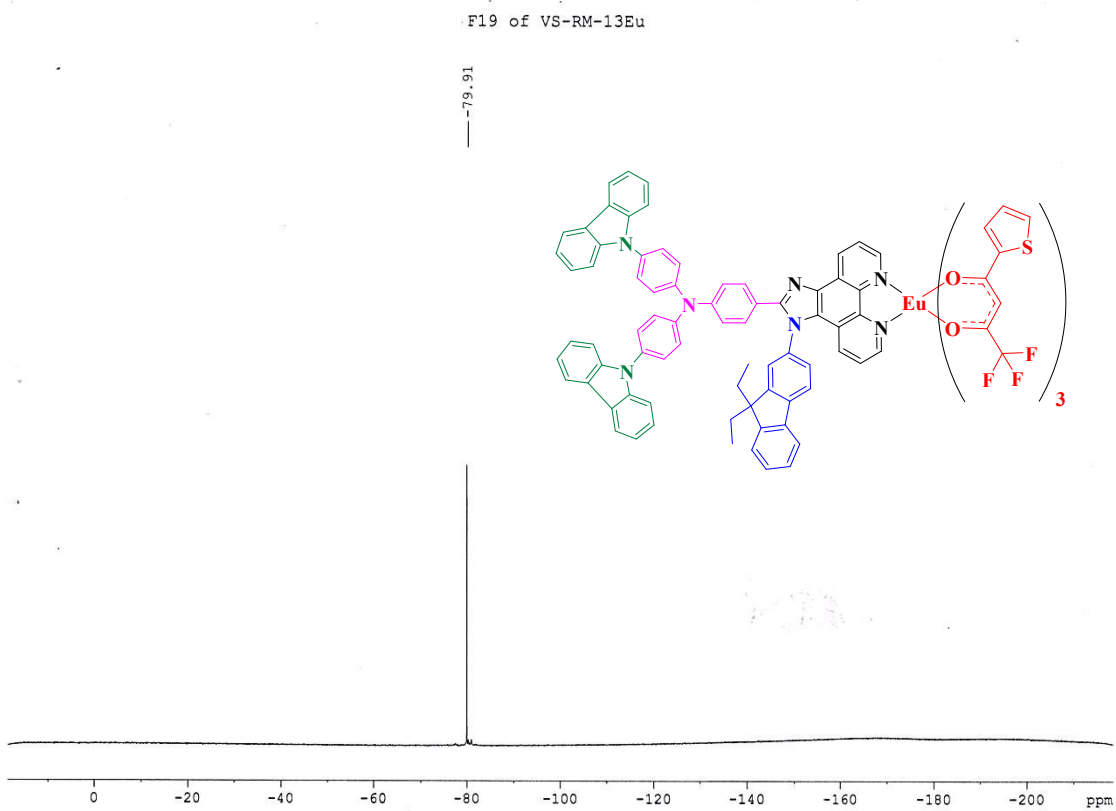
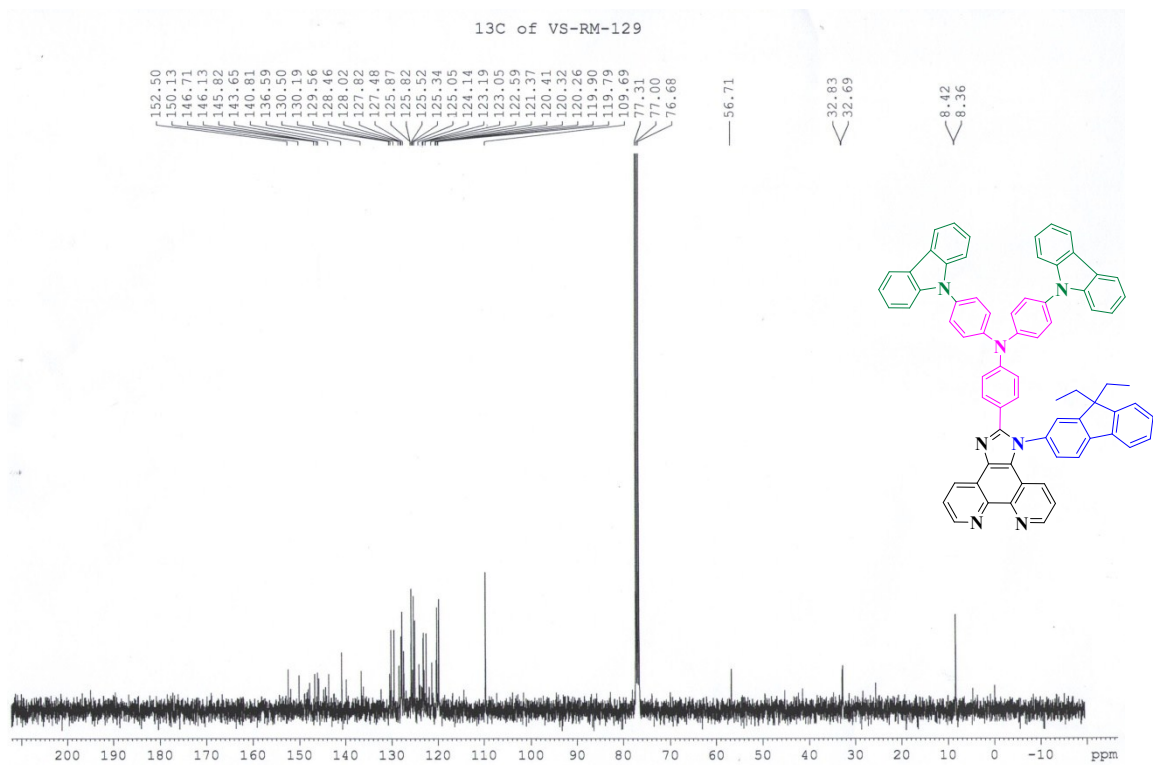


Phen-FI-TPA-CBZ

Fig. S1 ground state optimized structures of the ligand.

Fig. S2 ^1H (up), ^{13}C (middle) and ^{19}F -NMR (down) of Phen-FI-TPA-CBZ ligand.





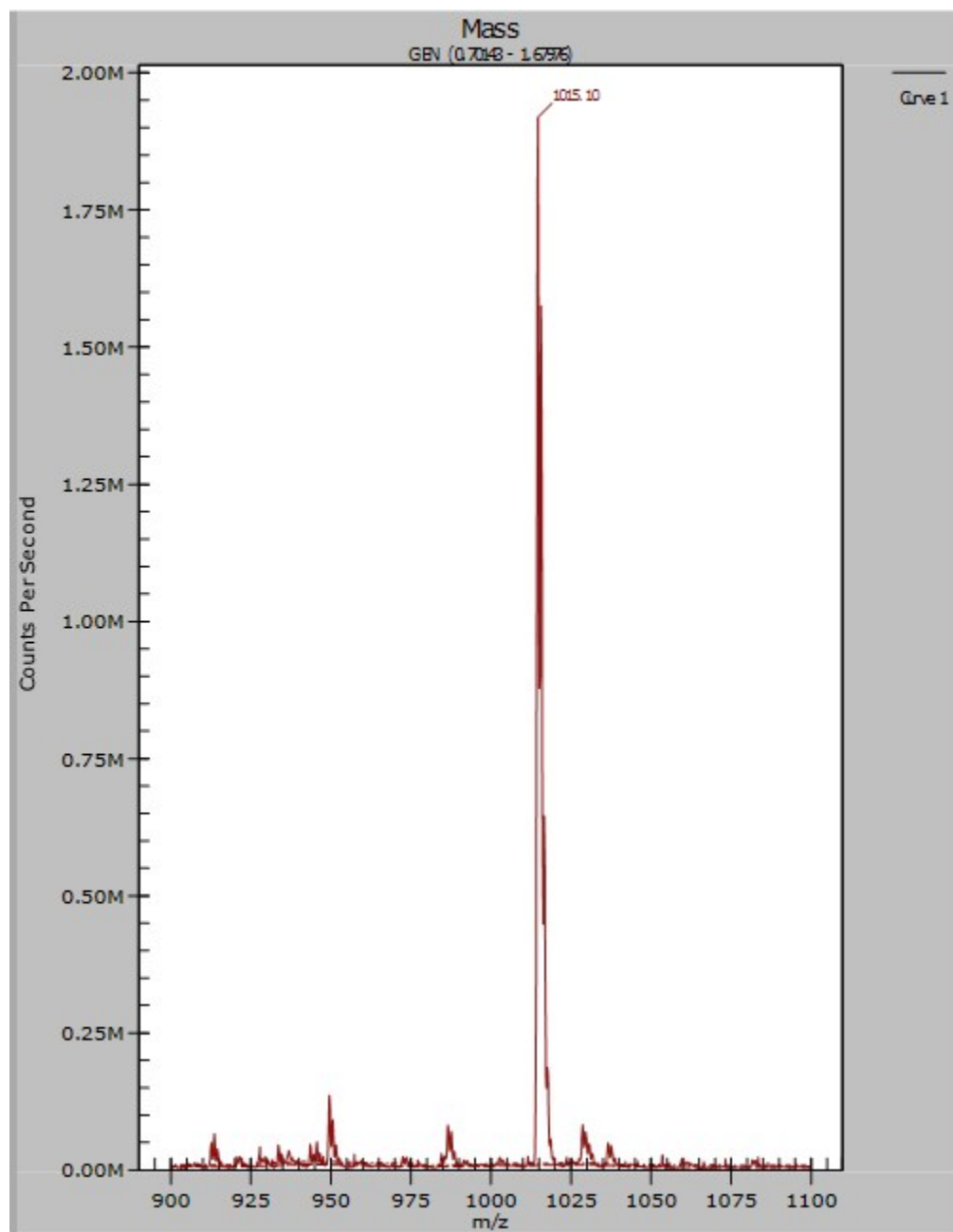


Fig. S3 The mass spectrum of the ligand, Phen-Fl-TPA-CBZ.

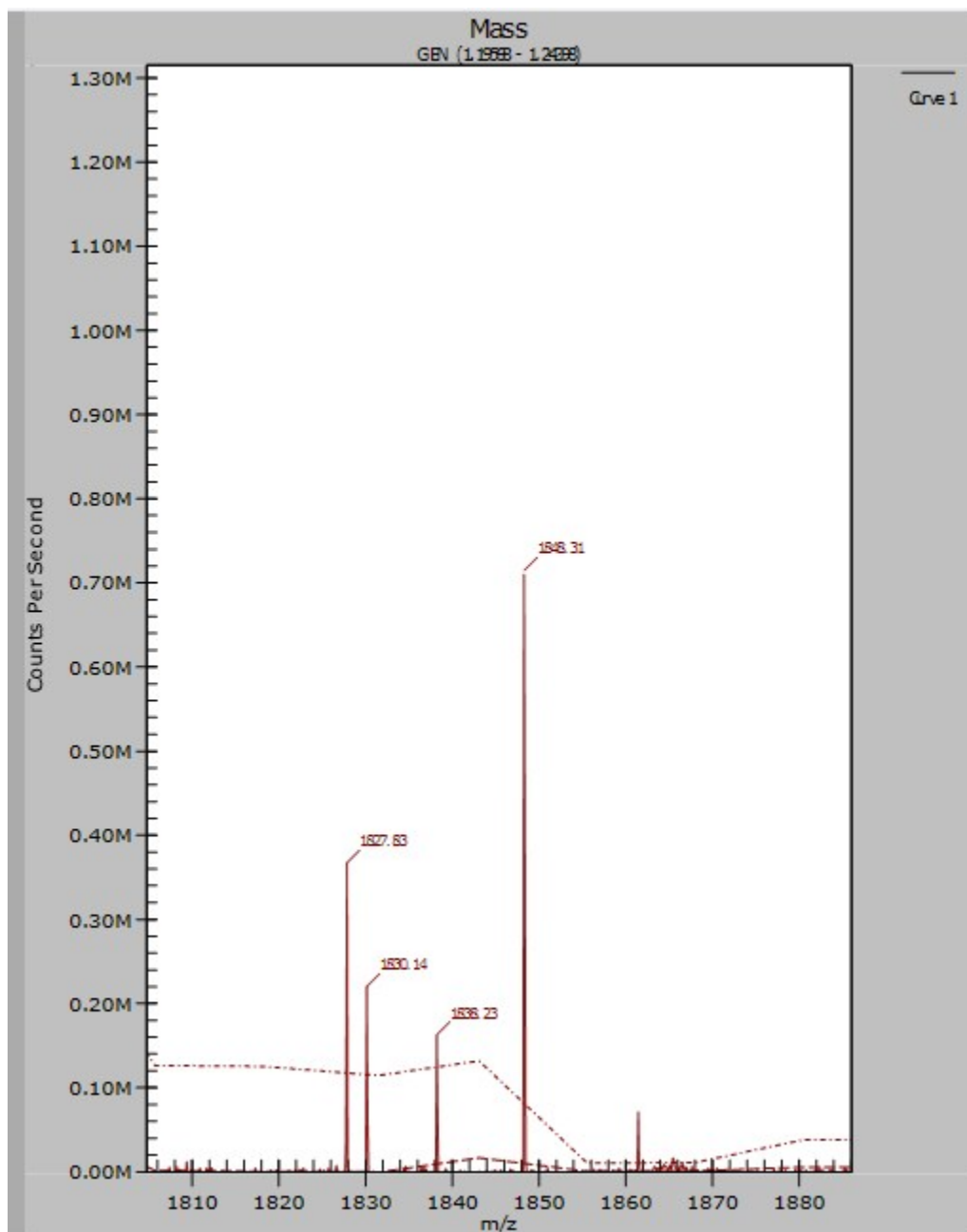


Fig. S4 The mass spectrum of the complex, $\text{Eu}(\text{TTA})_3\text{Phen-Fl-TPA-CBZ}$.

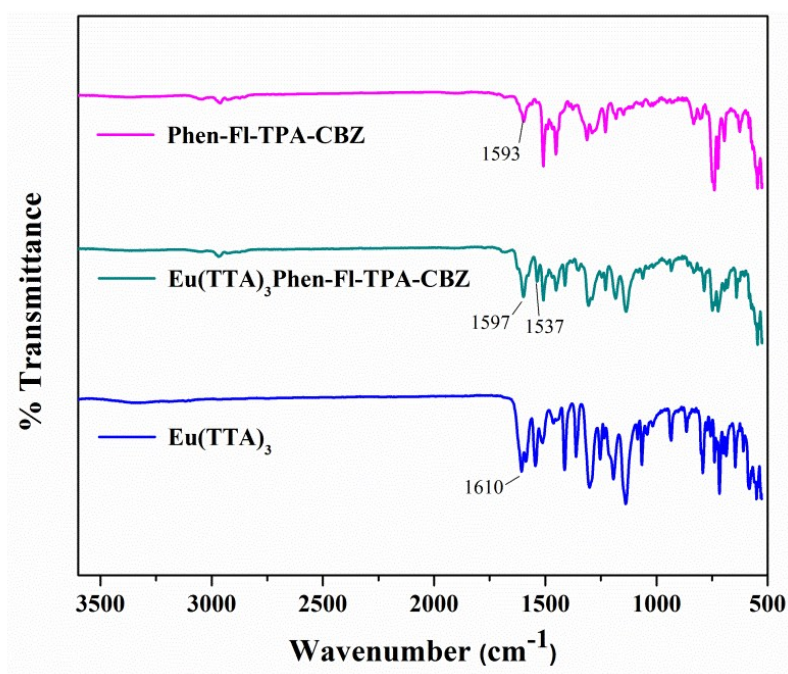


Fig. S5 FT-IR spectra of the ligand, corresponding Eu(III)-complex and $\text{Eu}(\text{tta})_3(\text{H}_2\text{O})_2$.

Table ST1 The foremost Infrared frequencies (wavenumber in cm^{-1}) at room temperature for free ligand, its corresponding Eu(III)-complex and $\text{Eu}(\text{tta})_3(\text{H}_2\text{O})_2$.

(Wavenumber in cm^{-1})	$\text{Eu}(\text{TTA})_3\text{Phen-FI-TPA-CBZ}$	Phen-FI-TPA-CBZ	$\text{Eu}(\text{tta})_3(\text{H}_2\text{O})_2$
$\nu(\text{C=O})$	1597	--,--	1610
$\nu(\text{C=N})$	1537	1593	--,--
$\nu(\text{C-N})$	1231	1227	--,--
$\nu(\text{C-F})$	1303	--,--	1298
$\nu(\text{C-CF}_3)$	1137	--,--	1133
$\nu(\text{C-H phen})$	833, 723	830, 737	--,--

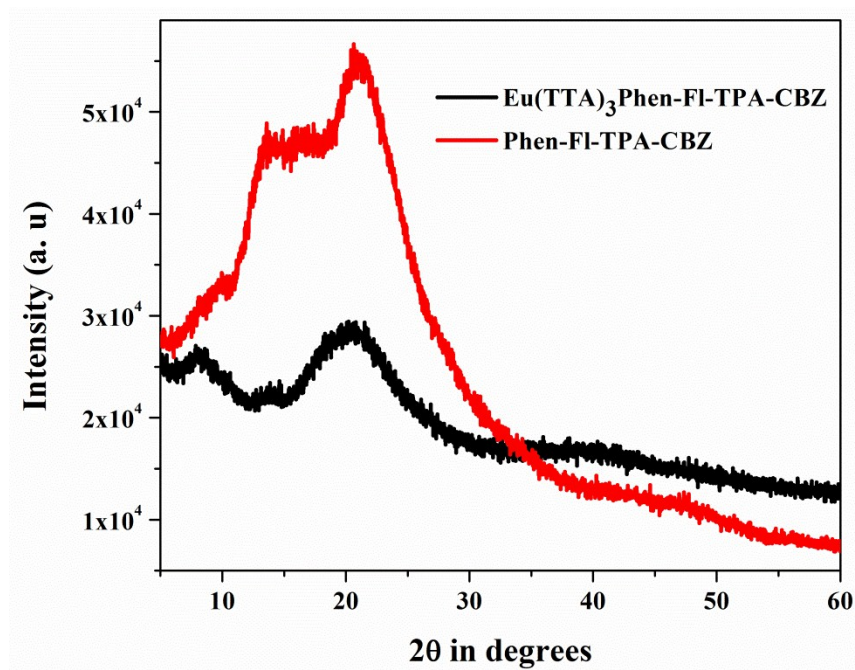


Fig. S6 The PXRD of the Phen-FI-TPA-CBZ ligand and corresponding Eu(III) complex.

ST2. The PXRD data's of Eu(III) complex.

ST2. Eu(TTA)₃Phen-FI-TPA-CBZ

Peak list

No.	2-theta(deg)	d(ang.)	Height(cps)	FWHM(deg)	Int. I(cps deg)	Int. W(deg)	Asym. factor
1	8.44(11)	10.47(14)	2447(175)	5.4(2)	16404(807)	6.7(8)	2.2(3)
2	20.22(6)	4.389(13)	5951(273)	6.90(6)	48335(818)	8.1(5)	0.81(3)

The PXRD diffraction studies were carried out to evaluate the crystalline or amorphous nature of the ligand and corresponding Eu(III) complex. The PXRD results of the Eu(III) complex shows the amorphous structure. The interplanar distances (d) of Eu(TTA)₃Phen-FI-TPA-CBZ complex is shifted to higher value as compare to that of ligand (Table ST2).

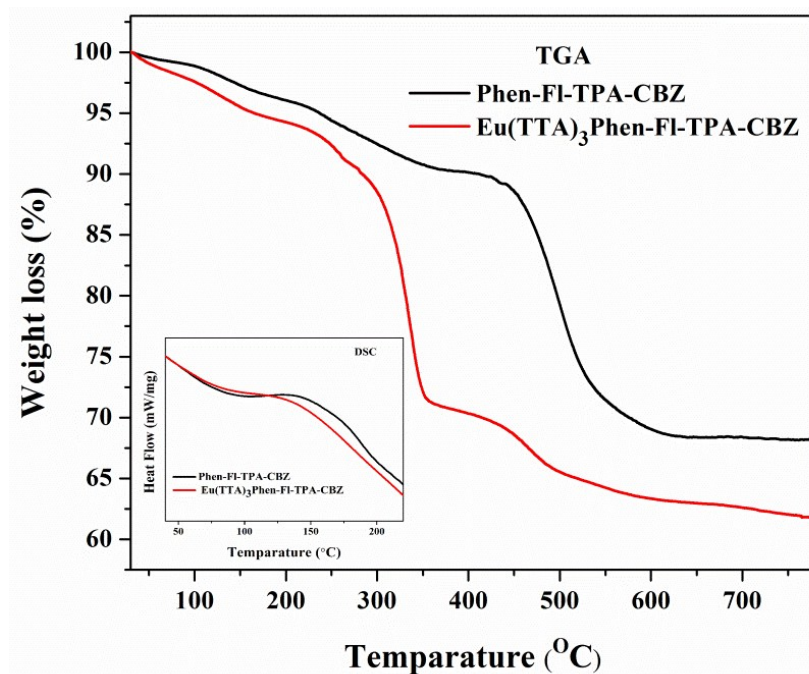


Fig. S7 TG- analysis curves for the ligand and its corresponding Eu(III) complex.

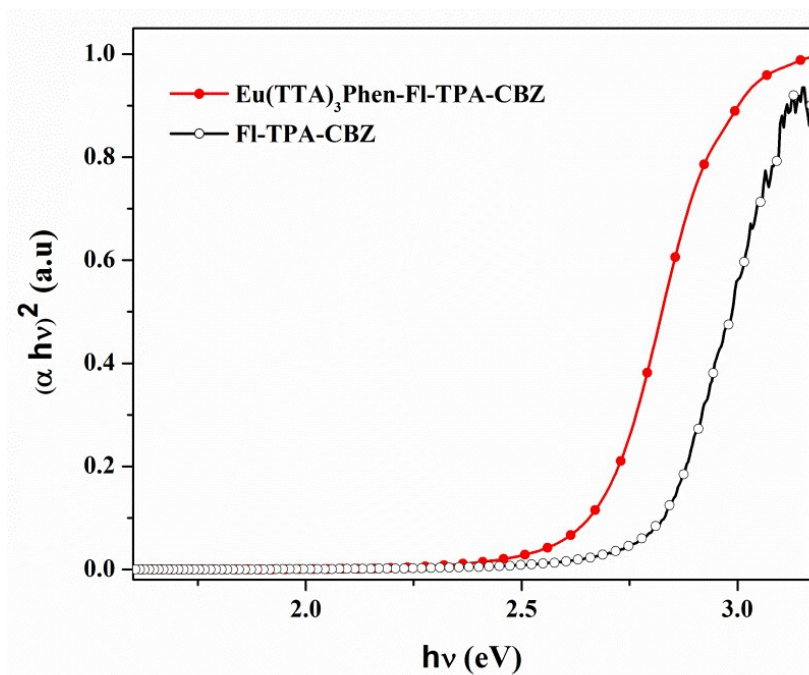


Fig. S8 The band gap for the ligands and their corresponding Eu (III) complexes are calculated from diffuse reflectance spectra

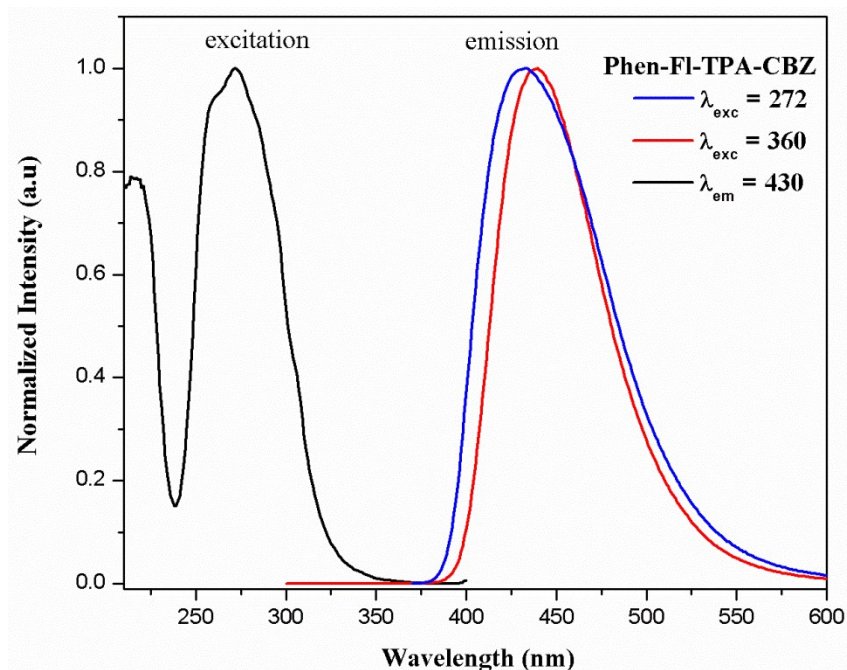


Fig. S9 The PL excitation and emission spectra of Phen-FI-TPA-CBZ with different excitation and emission wavelengths.

Solvatochromism : The solvatochromism of ligands emission spectra interpreted in terms of Lippert-mataga equation. It defines the Stokes shift in terms of the changes in dipole moment which occur upon excitation. According to the increasing the polarity of the solvent, there is a shift observed towards high wavelength is called red / batho chromic shift, which are showed in Fig.S10 (left and right). The equations (eq 2, 3) of Lippert–Mataga describes the solvatochromic Stokes shift $\bar{\Delta\nu}$ (expressed in wavenumbers) as a function of the change of the dipole moment $\Delta\mu_{ge} = \mu_e - \mu_g$ of the dye. The several solvents are performed by eq-2 with dissimilar dielectric constants (ϵ) and refractive indices (n) and by plotting $\bar{\Delta\nu}$ as a function of Δf .

$$\bar{\Delta\nu} = \frac{2\Delta f}{4\pi\epsilon_0 h c a^3} (\mu_e - \mu_g) + \text{constant} \quad \dots\dots\dots 2$$

$$f(\epsilon) = \frac{f(\epsilon - 1)}{f(2\epsilon + 1)} \quad \text{and} \quad f(n^2) = \frac{(n^2 - 1)}{(2n^2 + 1)} \quad \dots\dots\dots 3$$

$\bar{\Delta\nu} = \bar{\Delta\nu}_{\text{abs}} - \bar{\Delta\nu}_{\text{em}}$ is the solvatochromic shift (in cm^{-1}) between the maxima of absorption and fluorescence emission [$\bar{\Delta\nu}_{\text{abs}} = 1/\lambda_{\text{abs}} (\text{max})$, $\bar{\Delta\nu}_{\text{em}} = 1/\lambda_{\text{em}} (\text{max})$], h is Planck's constant, c is the velocity of light, ϵ_0 is the permittivity of vacuum (signifies the radius of the cavity in which the solute resides), μ_e , μ_g are dipolemoments in the excited and ground states.

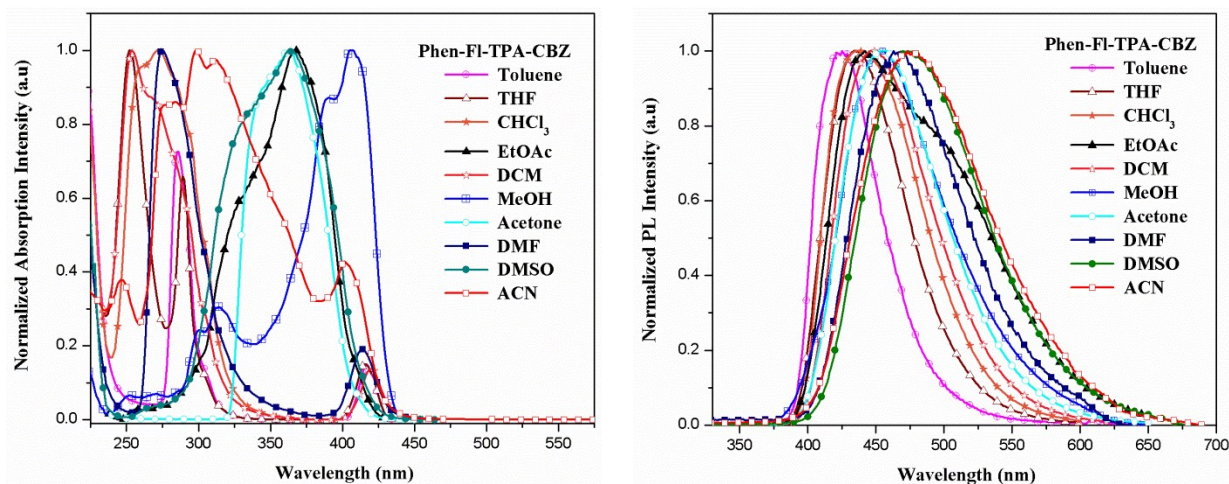


Fig. S10 The solvent effect of Phen-FI-TPA-CBZ of PL excitation (left) and emission (right) in different solvents.

Fig. S10 (left and right) were represents the Lippert–Mataga plot for Phen-FI-TPA-CBZ in the solvents listed in Table ST3. The Fig.S11 indicating that the linear relationship [correlation coefficient $r = 0.218$, slope = $(29.494) \times 10^3 \text{ cm}^{-1}$, intercept = $(5.010) \times 10^3 \text{ cm}^{-1}$] of the Stoke's shift plotting $\bar{\Delta\nu}$ verses Δf for the 10 solvents of CBZ ligand.

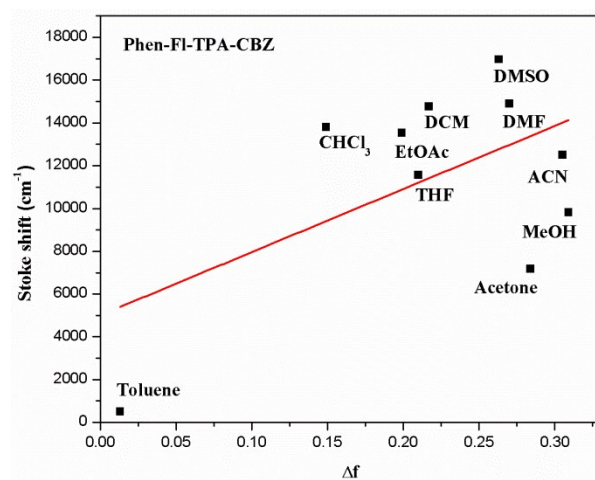


Fig. S11 Stoke's shift $\Delta\bar{\nu}$ of Phen-FI-TPA-CBZ (right) versus the Lippert solvent parameter $\Delta f = f(\epsilon) - f(n^2)$ (The numbers refer to the solvents in Table S1). The straight line represents the linear fit to the 10 data points.

Table ST3 PL spectral data of ligands in various solvents.

S. No.	λ_{abs} (max) (nm)	λ_{em} (max) (nm)	Stoke's shift ($\Delta\nu$) (cm^{-1})
	Phen-FI-TPA-CBZ	Phen-FI-TPA-CBZ	Phen-FI-TPA-CBZ
Toulene	416	425	509
DCM	270	449	14765
THF	289	434	11561
CHCl ₃	273	438	13799
EtOAc	255	441	13540
MeOH	314	454	9821
Acetone	343	455	7176
ACN	298	475	12518
DMF	275	466	14904
DMSO	263	475	16970

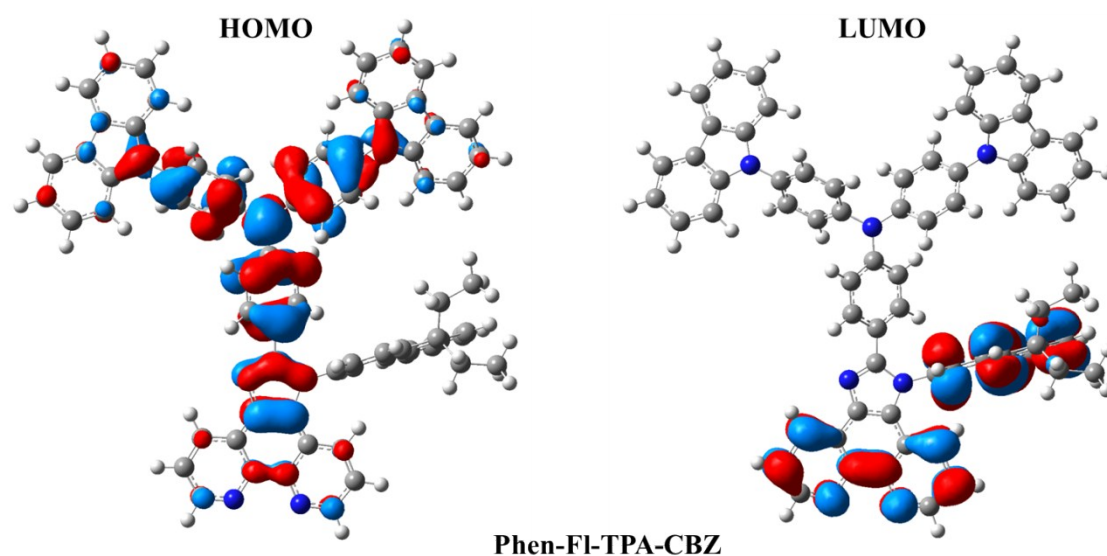


Fig. S12 The obtained HOMO-LUMO of the ligand.

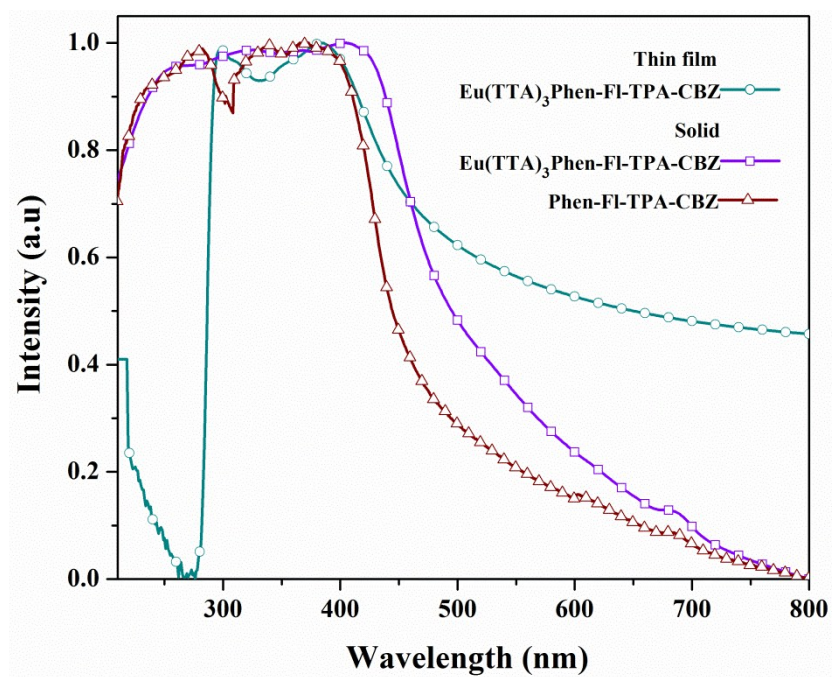


Fig. S13 The UV-Vis absorption spectra of $\text{Eu(TTA)}_3\text{Phen-FI-TPA-CBZ}$ and its ligand in thin

film and solid.

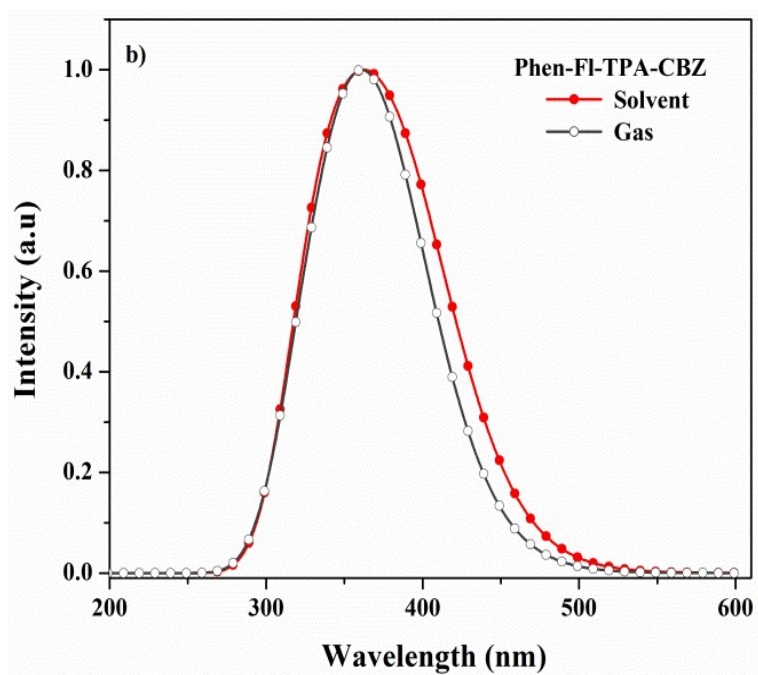


Fig. S14 The Phen-FI-TPA-CBZ ligand absorption spectra theoretically calculated.

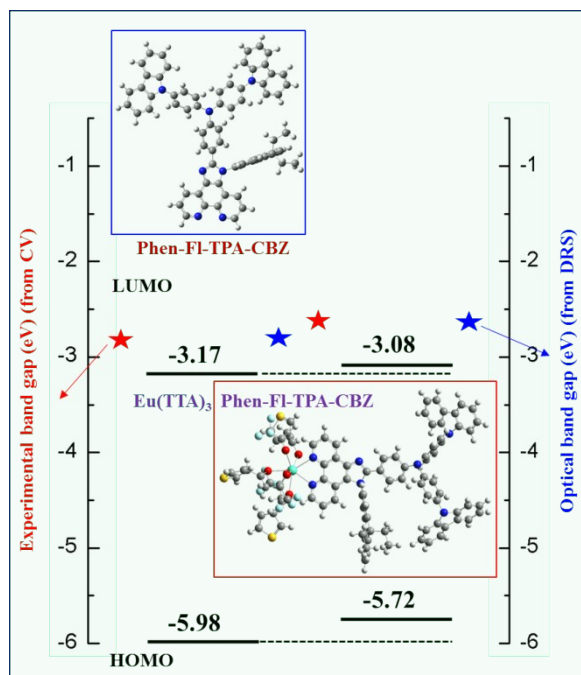


Fig. S15 The energy levels of the ligand as well as Eu(III) complex arrangement.

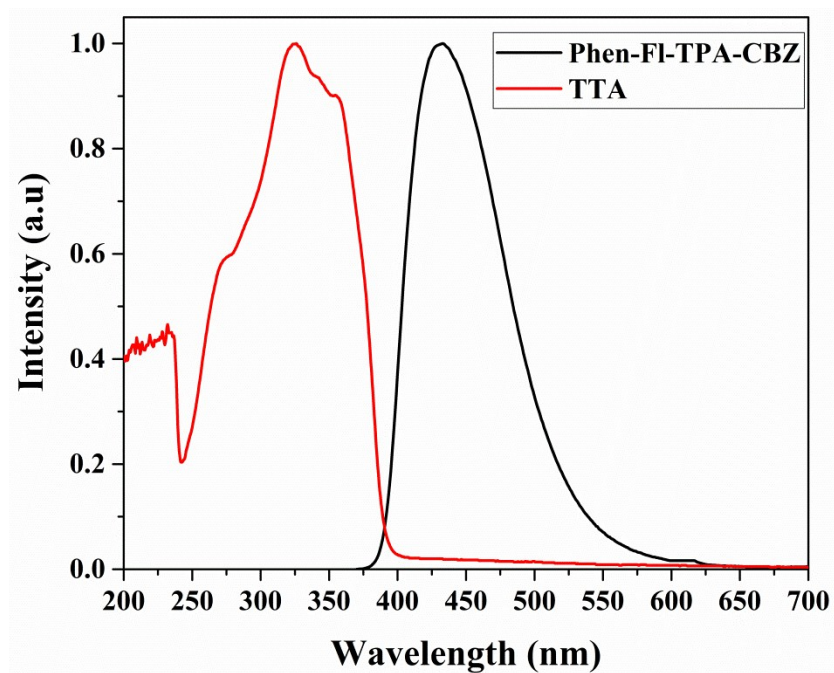


Fig. S16 The emission of the ligand (Phen-FI-TPA-CBZ) and UV-vis absorption spectra of TTA at Room-temperature.

References

- [1] .T. Wing, N. Mary, P.A. Matthew, P.K. Stuart, V. Panagiotis, M.K. Stephen, *Chemistry of Materials* 19 (2007) 5475.
- [2] K.D. Belfield, K.J. Schafer, W. Mourad, B.A. Reinhardt, *J. Org. Chem.* 65 (2000) 4475.
- [3] R. Abbel, C. Grenier, M.J. Pouderoijen, J.W. Stouwdam, P.E.L.G. Leclere, R.P. Sijbesma, E.W. Meijer, A.P.H.J. Schenning, *J. Am. Chem. Soc.* 131 (2009) 833.
- [4] W. Xu, B. Peng, J. Chen, M. Liang, F. Cai, *J. Phys. Chem. C* 112 (2008) 874.